Iodine Charge-Transfer Salts of Benzene-Bridged Bis(1,2,3,5-diselenadiazolyl) Diradicals. Electrocrystallization and Solid-State Characterization of 1,3- and 1,4-[(Se_2N_2C)C_6H_4(CN_2Se_2)][I]

C. D. Bryan,[1a] A. W. Cordes,*,[1a] N. A. George,[1b] R. C. Haddon,*,[1c] C. D. MacKinnon,[1b] R. T. Oakley,*,[1b] T. T. M. Palstra,[1c] and A. S. Perel[1c]

Department of Chemistry and Biochemistry, University of Arkansas, Fayetteville, Arkansas 72701; Guelph-Waterloo Centre for Graduate Work in Chemistry, Guelph Campus, Department of Chemistry and Biochemistry, University of Guelph, Guelph, Ontario N1G 2W1, Canada; and AT&T Bell Laboratories, 600 Mountain Ave., Murray Hill, New Jersey 07974

Received September 21, 1995. Revised Manuscript Received December 21, 1995[⊗]

Electroreduction of 1,3- and 1,4-benzene-bridged bis(diselenadiazolium) salts [1,4-Se][SbF_6]$_2$ and [1,4-Se][SbF_6]$_2$ in acetonitrile, at a Pt wire and in the presence of iodine affords the 1:1 charge-transfer salts [1,4-Se][I] and [1,3-Se][I]. Crystals of [1,4-Se][I] belong to the monoclinic space group $C2/m$, with FW = 598.9, a = 10.586(2), b = 16.713(2), c = 3.5006(14) Å, β = 104.26(2)°, V = 600.2(3) Å^3, Z = 2. Crystals of [1,3-Se][I] belong to the orthorhombic space group $Ima2$, with FW = 598.9, a = 28.489(7), b = 3.543(2), c = 12.283(2) Å, V = 1239.8(8) Å^3, Z = 4. In the presence of an excess of iodine, electrocrystallization of [1,4-Se]$^{2+}$ affords the mixed iodide/triiodide salt [1,4-Se][I][I_3], space group $C2/c$, FW = 979.59, a = 12.862(3), b = 15.063(2), c = 9.028(3) Å, β = 100.62(2)°, V = 1719.1(7) Å^3, Z = 4. The structures of the two 1:1 compounds consist of perfectly superimposed stacks of molecular units interspersed by columns of disordered iodines. Interstack contacts in both structures are limited, indicative of 1-dimensional electronic structures. Variable-temperature single-crystal conductivity measurements on [1,4-Se][I] reveal weakly metallic behavior at room temperature, with a phase transition to a semiconducting state occurring at about 240 K. Magnetic susceptibility measurements on [1,4-Se][I] are consistent with the conductivity data; the magnetic susceptibility of [1,3-Se][I] behaves similarly. The crystal structures and transport properties are discussed in light of extended Hückel band structure calculations.

Introduction

As part of our studies on the use of neutral π-radicals as building blocks for molecular conductors,[2−4] we recently reported the preparation, structures, and transport properties of iodine-doped charge-transfer (CT) salts of the benzene-bridged bis(dithiadiazolyl) diradicals [1,4-S] and [1,3-S] (**1** and **2**, E = S).[5,6] The

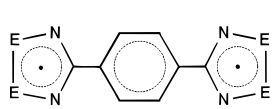

1

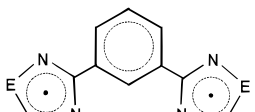

2

structures of [1,4-S][I] and [1,3-S][I] consist of perfectly superimposed and evenly spaced molecular units, interspersed with columns of disordered iodines. Both compounds exhibit metallic conductivity at ambient temperatures, but at lower temperatures charge density wave (CDW) driven instabilities cause the structures to collapse into semiconducting states. The susceptibility of the uniformly spaced stacks to undergo these CDW distortions was attributed to their 1-dimensional electronic structures. In the case of [1,4-S][I] the nature of the charge density state was characterized by low-temperature X-ray diffraction, and from these measurements the degree of bandfilling (f = $^3/_8$) was determined. A simple model of the consequent superlattice was proposed.

Suppression of the metal−insulator transition in these stacked CT salts requires the design of materials with more 2- and 3-dimensional electronic structures. In light of the known effectiveness of intermolecular chalcogen−nitrogen (E- - -N) and chalcogen−chalcogen (E- - -E) to increase the dimensionality of molecular

⊗ Abstract published in *Advance ACS Abstracts,* February 15, 1996.

(1) (a) University of Arkansas. (b) University of Guelph. (c) AT&T Bell Laboratories.

(2) Bryan, C. D.; Cordes, A. W.; Haddon, R. C.; Glarum, S. H.; Hicks, S. H.; Kennepohl, D. K.; MacKinnon, C. D.; Oakley, R. T.; Palstra, T. T. M.; Perel, A. S.; Schneemeyer, L. F.; Scott, S. R.; Waszczak, J. V. *J. Am. Chem. Soc.* **1994**, *116*, 1205.

(3) Bryan, C. D.; Cordes, A. W.; Haddon, R. C.; Hicks, R. G.; Oakley, R. T.; Palstra, T. T. M.; Perel, A. S.; Scott, S. R. *Chem. Mater.* **1994**, *6*, 508.

(4) Bryan, C. D.; Cordes, A. W.; Goddard, J. D.; Haddon, R. C.; Hicks, R. G.; Mackinnon, C. D.; Mawhinney, R. C.; Oakley, R. T.; Palstra, T. T. M.; Perel, A. S. *J. Am. Chem. Soc.*, in press.

(5) Bryan, C. D.; Cordes, A. W.; Fleming, R. M.; George, N. A.; Glarum, S. H.; Haddon, R. C.; MacKinnon, C. D.; Oakley, R. T.; Palstra, T. T. M.; Perel, A. S. *J. Am. Chem. Soc.* **1995**, *117*, 6880.

(6) Bryan, C. D.; Cordes, A. W.; Fleming, R. M.; George, N. A.; Glarum, S. H.; Haddon, R. C.; Oakley, R. T.; Palstra, T. T. M.; Perel, A. S.; Schneemeyer L. F.; Waszczak, J. V. *Nature* **1993**, *365*, 821.

0897-4756/96/2808-0762$12.00/0

materials,[7,8] we are pursuing the design of modifications of **1** and **2** that will lead to enhanced intermolecular contacts in the solid state. On the basis of the belief that intermolecular interactions should be stronger for selenium than sulfur, we have prepared and characterized iodine CT salts of the diselenadiazolyl derivatives [1,4-Se] and [1,3-Se] (**1** and **2**, E = Se). In the present paper we report the crystal structures and transport properties of these compounds. The structures and behavior of the sulfur- and selenium-based systems [1,4-E][I] and [1,3-E][I] (E = S, Se) are compared and discussed in the light of extended Hückel band calculations.

Results and Discussion

Electrocrystallization of Salts. The iodine-doped dithiadiazolyl CT salts reported to date have all been prepared by thermal methods. Typically the native radical or diradical is cosublimed in the presence of iodine. Alternatively, the two reagents can be allowed to react in an inert solvent, such as benzonitrile, and the crude salt so formed sublimed in a static vacuum to afford pristine crystalline material. This approach fails for the selenium based diradicals [1,4-Se] and [1,3-Se]. Although the two compounds react cleanly with iodine in benzonitrile at 130 °C, to afford crude products which, by mass balance, appear to be 1:1 CT salts, sublimation in vacuo fails; the compounds decompose at about 240 K without sublimation.

As an alternative method to producing selenium-based CT salts, we have investigated electrocrystallization, a technique widely used for the generation of radical ion salts. We have found that the dications $[1,4\text{-Se}]^{2+}$ and $[1,3\text{-Se}]^{2+}$ (as their hexafluoroantimonate salts), when dissolved in acetonitrile and in the presence of iodine, can be electroreduced at a Pt wire electrode to afford needlelike crystals of the CT salts [1,4-Se][I] and [1,3-Se][I]. These salts grow as fine, hairlike needles. However, with currents of $<5\ \mu$A and growth periods of 10−14 days, material with dimensions sufficient for single-crystal measurements can be prepared. For the 1,3 derivative, the relative concentration of iodine (varied from 2-fold to 10-fold excess) appeared to have little effect on the quality or nature of the crystals of the resultant [1,3-Se][I]. In the case of the 1,4 derivative, however, the use of a 10-fold excess of iodine afforded a second, blocklike phase of composition [1,4-Se][I][I_3]. The structures of all these electrocrystallized materials are described below.

Crystal Structure of [1,4-Se][I]. Crystals of [1,4-Se][I] belong to the monoclinic space group *C*2/*m*. Atomic coordinates are listed in Table 1, and pertinent intramolecular bond distances are summarized in Table 2. The crystal structure (Figure 1) is similar to that recently reported for [1,4-S][I] (space group *Immm*), i.e., perfectly superimposed stacks of molecules uniformly spaced at a distance of 3.5016(1) Å (cf. 3.415(2) Å in [1,4-S][I]). Viewed down the stacks the molecules are arranged in ribbons bridged by (disordered) iodine atoms. In adjacent ribbons the CN_2Se_2 rings are interlocked in a "dovetailed" arrangement. In contrast to [1,4-S][I], in which the molecule is bisected by three mutually perpendicular mirror planes, the structure of [1,4-Se][I] lies on a single mirror plane that bisects the benzene ring. The molecular unit, however, is not planar; the benzene ring is twisted away from the plane

Table 1. Atomic Parameters *x*, *y*, *z*, and B_{eq} for [1,4-Se][I], [1,3-Se][I], and [1,4-Se][I][I_3] (ESDs Refer to the Last Digit Printed)

[1,4-Se][I]

	x	*y*	*z*	B_{eq}	occupancy
I1	0	0	0	8.8 (11)	0.35007
I2	0.0034(8)	0	0.115(3)	4.2(3)	0.32496
Se	0.88774(5)	0.18449(3)	0.42878(20)	2.89(3)	
N	0.8837(4)	0.2908(3)	0.4241(15)	2.62(21)	
C1	1	0.3280(5)	1/2	2.4(3)	
C2	1	0.4154(5)	1/2	2.0(3)	
C3	1.1112(5)	0.4599(4)	0.6741(18)	2.39(21)	
H3	1.189	0.432	0.796	3.1	

[1,3-Se][I]

	x	*y*	*z*	B_{iso}/B_{eq}	occupancy
I1	1/2	0	0.00000	8.0(3)	0.46
I2	0.50000	0.151(17)	0.00000	6.6(9)	0.27
Se1	0.88962(9)	0.1774(8)	0.4172(4)	3.13(11)	
Se2	0.92978(9)	0.1613(10)	0.2533(3)	3.44(12)	
N1	0.8355(7)	0.126(5)	0.3481(16)	2.6(4)	
N2	0.8773(7)	0.106(5)	0.1796(18)	3.1(4)	
C1	0.8386(8)	0.086(6)	0.2410(16)	1.9(4)	
C2	0.7915(8)	0.032(8)	0.1858(18)	2.3(4)	
C3	0.7914(8)	−0.099(7)	0.0792(20)	2.5(4)	
C4	3/4	−0.167(11)	0.028(3)	2.8(6)	
C5	3/4	0.103(9)	0.2354(24)	2.2(6)	
H3	0.819	−0.186	0.043	3.3	
H4	3/4	−0.270	−0.043	3.6	
H5	3/4	0.196	0.308	2.9	

[1,4-Se][I][I_3]

	x	*y*	*z*	B_{eq}	occupancy
I1	1/2	0.06820(16)	1/4	3.66(10)	
I2	1/4	1/4	0	6.0(15)	0.27551
I3	0.047(3)	0.2727(10)	0.1717(23)	12.6(27)	0.33549
I4	0	0.2719(15)	1/4	9.3(17)	0.31460
I5	0.092(5)	0.2781(22)	0.151(3)	14.6(23)	0.28720
I6	0.2062(15)	0.2593(9)	0.0593(15)	6.1(15)	0.29485
I7	0.1583(20)	0.2628(15)	0.1142(17)	8.4(17)	0.28740
Se1	0.69996(19)	0.14291(15)	0.0786(3)	3.71(11)	
Se2	0.68597(17)	−0.00668(15)	0.0437(3)	3.02(9)	
N1	0.8024(13)	0.1494(11)	−0.0272(18)	2.7(3)	
N2	0.7896(11)	−0.0062(11)	−0.0574(17)	2.3(3)	
C1	0.8356(15)	0.0704(14)	−0.0784(22)	2.7(4)	
C2	0.9207(12)	0.0709(12)	−0.1692(18)	1.4(3)	
C3	0.9605(13)	−0.0081(12)	−0.2073(20)	1.8(3)	
C4	0.9632(13)	0.1510(12)	−0.2064(19)	1.7(3)	
H3	0.934	−0.063	−0.176	2.6	
H4	0.940	0.205	−0.170	2.5	

[a] B_{eq} is the mean of the principal axes of the thermal ellipsoid. Only those occupancy factors determined by least-squares refinement are shown.

Table 2. Pertinent Intramolecular Distances (Å) (Mean Values, ESDs or Range in Parentheses)

	Se−Se	Se−N
$[1,4\text{-Se}]_2$[a]	2.338(19)	1.79(3)
[1,4-Se][I]	2.305(1)	1.778(6)
$[1,3\text{-Se}]_2$[b]	2.35(30)	1.78(11)
[1,3-Se][I]	2.316(6)	1.76(2)
[1,4-Se][SbF_6]·3PhCN[c]	2.259(12)	1.725(19)
[1,4-Se][I][I_3]	2.278(3)	1.76(2)

[a] Reference 14. [b] References 16 and 17. [c] Reference 15.

(7) Cordes, A. W.; Haddon, R. C.; Oakley, R. T. In *The Chemistry of Inorganic Ring Systems*; Steudel, R., Ed.; Elsevier: New York, 1992; p 295.

(8) (a) Zambounis, J. S.; Christen, E.; Pfeiffer J.; Rihs, G. *J. Am. Chem. Soc.* **1994**, *116*, 925. (b) Suzuki, T.; Fukui, H.; Yamashita, Y.; Kabuto, C.; Tanaka, S.; Harasawa, M.; Mukui, T.; Miyashi, T. *J. Am. Chem. Soc.* **1992**, *114*, 3034. (c) Sandman, D. J. *Mol. Cryst. Liq. Cryst.* **1979**, *50*, 235. (d) Alcock, N. W. *Adv. Inorg. Radiochem.* **1972**, *15*, 1.

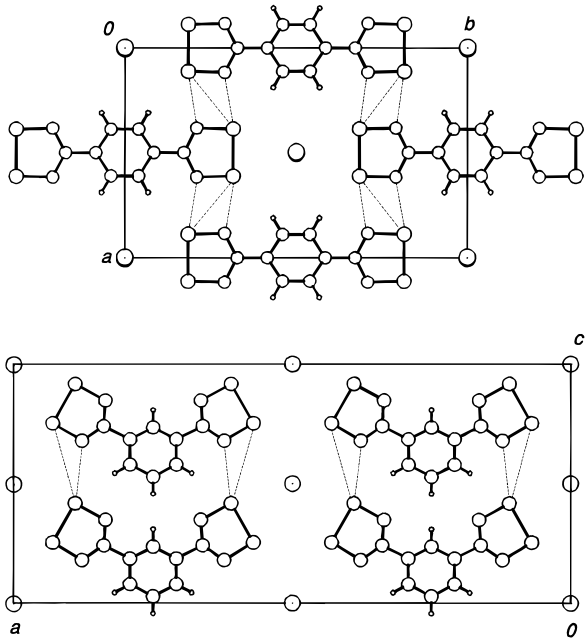

Figure 1. Packing of [1,4-Se][I] (top) and [1,3-Se][I] (bottom), viewed down thestacking direction. Intermolecular Se- - -Se and Se- - -N contacts are shown with dashed lines.

of the two CN_2Se_2 rings to make a dihedral angle of 17.3(9)°. While the packing pattern viewed down the stack is similar to that found for [1,4-S][I], the view in the *y* direction (Figure 2) reveals subtle but significant differences. In [1,4-S][I] adjacent ribbons running parallel to *y* are perfectly out-of-register, i.e., equal contacts up and down to either side. The intermolecular S- - -S contacts (3.911(1) Å) are somewhat longer than the van der Waals separation (3.6 Å),[9] but the corresponding S- - -N distances (3.320(2) Å) are within the van der Waals separation (3.35 Å). In [1,4-Se][I], the displacement of adjacent ribbons is less symmetric; there are now two lateral Se- - -Se contacts (3.777(1) and 4.243(1) Å) (Figure 2) and two lateral Se- - -N contacts (3.069(4) and 3.621(5) Å) that link the molecular units in an extended manner in the *x* direction. These distances can be compared with values of 3.8 and 3.45 Å for the respective Se- - -Se and Se- - -N van der Waals separations.[9]

The iodine atoms are disordered along the *z* direction, but the fractional occupancies (0.33) of the two iodine positions used in the disorder model suggest that there is no disorder along a single stack. The iodines cluster into weakly associated, symmetric triiodides centered (I1) at, for example, 0,0,0. Within each triodide the I−I distance is 3.107 Å, significantly longer than in the triiodide unit observed in $[PhCN_2Se_2]_3[I_3]$ (mean d(I−I) = 2.909 Å),[3] as well as discrete triiodides, e.g., $Ph_4As^+ I_3^-$ (2.920Å),[10] but within the general range (3.1−3.3 Å) found for other linear chain triiodides.[11] While there appears to be order within a given chain of iodines, there is no order in the registry of adjacent chains.[12] There is no evidence for a larger repeat distance along *z*.

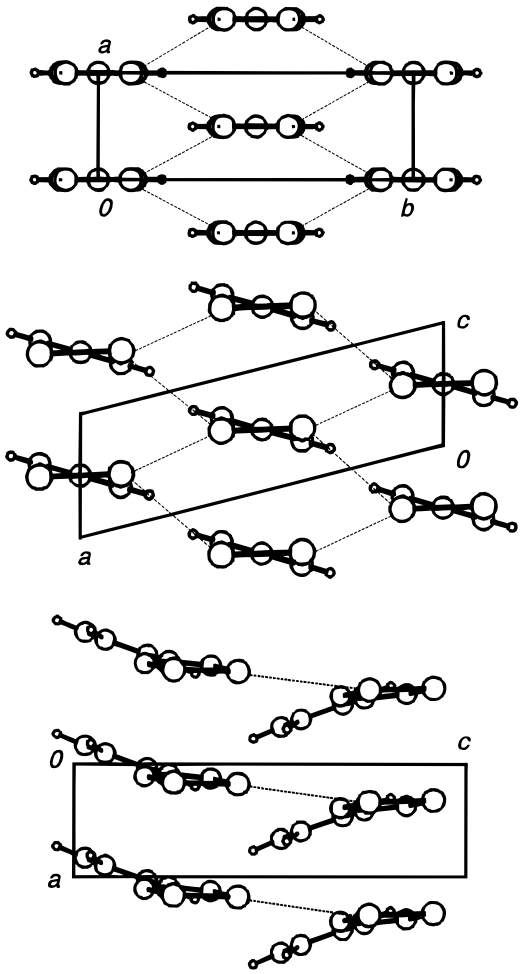

Figure 2. Stacking of rings in [1,4-S][I] (top), [1,4-Se][I] (middle), and [1,3-Se][I] (bottom). Iodine atoms are omitted for clarity.

Consistently with the standard MO description of the neutral radical, for which the singly occupied molecular orbital (SOMO) is the a_2 symmetry orbital π_4,[13] the

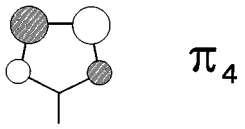

internal structural parameters of the heterocyclic rings in the CT salt [1,4-Se][I] (Table 2) are intermediate between those found in the neutral dimer $[1,4\text{-Se}]_2$[14] and the salt $[1,4\text{-Se}][SbF_6]_2 \cdot 3PhCN$, where the fully oxidized dication $[1,4\text{-Se}]^{2+}$ prevails.[15] As in the case of [1,4-S]-[I] the balance favors the neutral state, suggestive of less than a full positive charge on the molecule as a whole (less than $+^1/_2$ per ring).

Crystal Structure of [1,3-Se][I]. Crystals of [1,3-Se][I] are isomorphous with those of [1,3-S][I], belonging to the polar orthorhombic space group *Ima*2. Atomic

(9) Bondi, A. *J. Phys. Chem.* **1964**, *68*, 441.
(10) Runsink, J.; Swen-Walstra, S.; Migchelsen, T. *Acta Crystallogr.* **1972**, *B28*, 1331.
(11) Kertész, M; Vonderviszt, F. *J. Am. Chem. Soc.* **1982**, *104*, 5889.
(12) (a) Marks, T. J.; Kalina, D. W. *Extended Linear Chain Compounds* **1982**, *1*, 197. (b) Coppens, P. *Extended Linear Chain Compounds* **1982**, *1*, 333.
(13) Cordes, A. W.; Bryan, C. D.; Davis W. M., DeLaat, R. H.; Glarum, S. H.; Goddard, J. D.; Haddon, R. C.; Hicks, R. G.; Kennepohl, D. K.; Oakley, R. T.; Scott S. R.; Westwood, N. P. C. *J. Am. Chem. Soc.* **1993**, *115*, 7232.
(14) Cordes, A. W.; Haddon, R. C.; Oakley, R. T.; Schneemeyer, L. F.; Waszczak, J. A.; Young, K. M;. Zimmerman, N. M. *J. Am. Chem. Soc.* **1991**, *113*, 582.
(15) Cordes, A. W.; Oakley, R. T. *Acta Crystallogr.* **1990**, *C46*, 699.

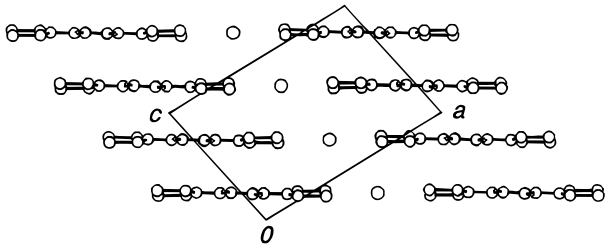

Figure 3. Packing of layers in [1,4-Se][I][I_3]. Ribbons of dications are linked by iodides.

coordinates are listed in Table 1 and pertinent intramolecular bond distances are summarized in Table 2. This structure also consists of perfectly superimposed stacks of molecules interspersed by columns of disordered iodines. As in the case of [1,4-Se][I], comparison of the internal structural parameters of [1,3-Se][I] with those of the neutral dimer $[\mathbf{3}]_2$[16,17] (Table 2) indicate an oxidation state of less than $+^1/_2$ per ring. Viewed down the stacking direction (Figure 1) the characteristic "nested spoons" packing is observed. In contrast to the 1,4 derivatives, adjacent stacks in [1,3-S][I] and [1,3-Se][I] are almost completely in-register (Figure 2). As noted for [1,3-S][I], this arrangement is not particularly conducive to short interstack Se- - -Se contacts that are critical to the development of a 2- or 3-dimensional electronic structure. For example, the closest lateral intercolumnar contact in the *z* direction, Se1- - -Se2′ (4.323(6) Å), is well outside the standard van der Waals contact (of 3.8 Å) (in [1,3-S][I] S1- - -S2′ is 4.53(2) Å). However, at 3.33(2) Å the Se1- - -N2′ distance is somewhat inside the van der Waals separation (3.45 Å) (in [1,3-S][I] S1- - -N2′ is 3.56(2) Å).

The molecular units in [1,3-Se][I] lie on a single mirror plane that bisects the benzene ring. As a whole the molecule is far from planar (Figure 2); the plane of the two CN_2Se_2 rings makes a dihedral angle of 16.7° with that of the benzene ring (in [1,3-S][I] this dihedral angle is 14.3°).

Crystal Structure of [1,4-Se][I][I_3]. Crystals of [1,4-Se][I][I_3] belong to the monoclinic space group *C*2/*c*. Atomic coordinates are listed in Table 1 and pertinent intramolecular bond distances are summarized in Table 2. The molecular unit, the $[1,4\text{-Se}]^{2+}$ dication, is bisected by a crystallographic 2-fold axis which lies in the plane of the benzene ring and is perpendicular to the long axis of the molecule. The plane of the CN_2Se_2 ring and that of the benzene ring are twisted so as to make a dihedral angle of 8.0(8)°. The crystal structure consists of ribbonlike arrays of $[1,4\text{-Se}]^{2+}$ dications linked by bridging iodides that are within 0.03(2) Å of the ring planes (Figure 3). That the CN_2Se_2 rings are discrete cations (i.e., fully oxidized) is readily apparent from the internal structural features; the Se−Se and Se−N distances are very similar to those observed in [1,4-Se][SbF_6]$_2$·3PhCN. Taken collectively, the ribbonlike arrays of alternating dications and iodides form

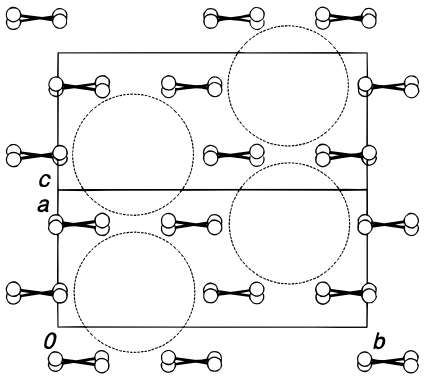

Figure 4. Pseudohexagonal cavities between ribbons [in 1,4-Se][I][I_3], which contain disordered polyiodide chains. For clarity, only Se atoms are shown.

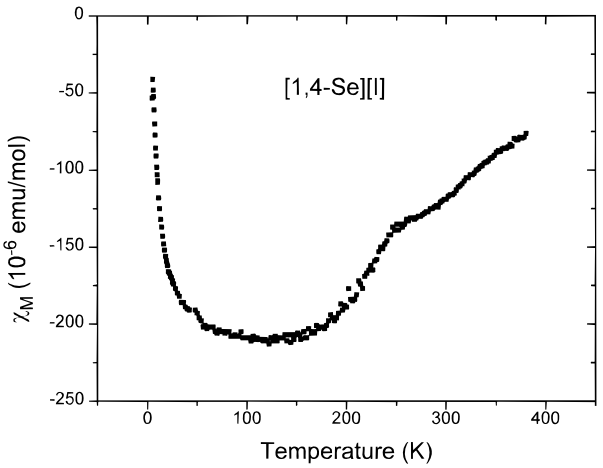

Figure 5. Magnetic susceptibilty of [1,4-Se][I] as a function of temperature.

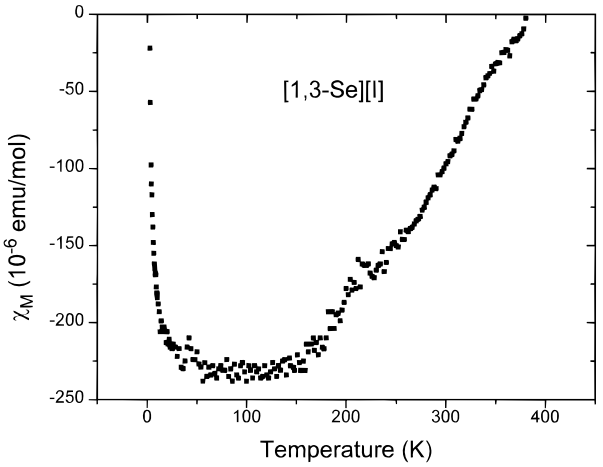

Figure 6. Magnetic susceptibilty of [1,3-Se][I] as a function of temperature.

bundles which, when viewed down the ribbons, take on the appearance of sets of hexagonal (close-packed) tubes (Figure 4). Inside these tubes or cavities lie disordered polyiodides. The multiplicative products of site multiplicity and occupancy factor for all the iodine residues combine to indicate 16 iodine atom equivalents/unit cell. Nominally, the iodine species within the cavity can be viewed as a triiodide. This would provide the correct charge balance with a $[1,4\text{-Se}]^{2+}$ dication.

Magnetic and Conductivity Measurements. Figures 5 and 6 shows the magnetic susceptibility behavior of the two 1:1 salts [1,4-Se][I] and [1,3-Se][I] as a

(16) (a) Andrews, M. P.; Cordes, A. W.; Douglass, D. C.; Fleming, R. M.; Glarum, S. H.; Haddon, R. C.; Marsh, P.; Oakley, R. T.; Palstra, T. T. M.; Schneemeyer, L. F.; Trucks, G. W.; Tycko, R. R.; Waszczak, J. V.; Warren, W. W.; Young, K. M.; Zimmerman, N. M. *J. Am. Chem. Soc.* **1991**, *113*, 3559.

(17) Cordes, A. W.; Haddon, R. C.; Hicks, R. G.; Oakley, R. T.; Palstra, T. T. M.; Schneemeyer, L. F.; Waszczak, J. V. *J. Am. Chem. Soc.* **1992**, *114*, 1729.

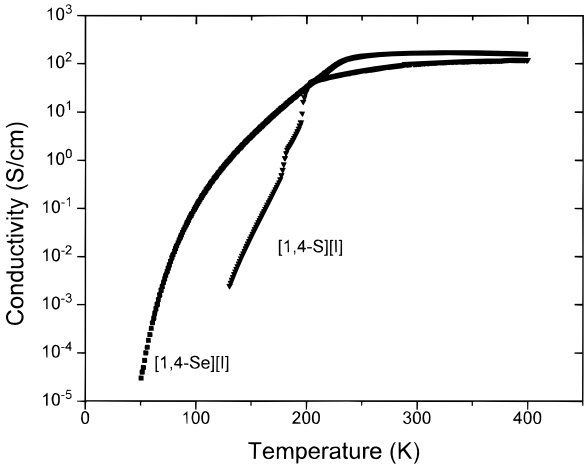

Figure 7. Conductivity of [1,4-Se][I] and [1,4-S][I] as a function of temperature.

function of temperature. The materials are basically diamagnetic insulators at low temperatures; a Curie fit to the data below 100 K led to susceptibilities of −205 and −237 cgs ppm mol^{-1} for the diamagnetic terms for [1,4-Se][I] and [1,3-Se][I], in good agreement with estimates based on the Pascal scheme. The concentrations of unpaired spins were found to be 0.09% and 0.14%, respectively. Paramagnetism develops in both materials near 200 K and continues to rise up to 400 K, the limit of the experiment.

Only in the case of [1,4-Se][I] were crystals large enough for four-probe single-crystal conductivity measurements. The single-crystal conductivity (along the needle axis) of [1,4-Se][I] is plotted in Figure 7 as a function of temperature. The results show that the transition seen in the magnetic measurement near 240 K corresponds to a metal-insulator transitions. The conductivity is activated in the low-temperature region; above 240 K the conductivity is weakly metallic. The highest conductivity attained is 200 S cm^{-1} at ca. 300 K.

Both the magnetic and conductivity measurements on these selenium-based materials are qualitatively in agreement with those obtained previously on the corresponding sulfur compounds. The conductivity of [1,4-Se][I] is higher than that of [1,4-S][I], but the metal/insulator transition temperature T_{MI} is also higher, near 240 K in the present case vs. 190 K for [1,4-S][I]. The higher conductivity of [1,4-Se][I] can be attributed to the expected better overlap along the stack between selenium as opposed to sulfur centers. However, the higher T_{MI} implies a less stable, more 1-dimensional electronic structure, an interpretation supported by the band structure calculations described below.

Band Structure Calculations. To assess the relative magnitude of orbital interactions between the CN_2E_2 molecules along and across the stacks of [1,4-E][I] and [1,3-E][I] (E = S, Se), we have carried out a series of extended Hückel band calculations on model assemblies related to the full crystal structures. We have focused on simplified 2-dimensional unit cells consisting of two adjacent HCN_2E_2 radicals located at the unit-cell positions provided by the X-ray data. The consequent 2-dimensional crystal orbitals (COs) are accordingly grouped into pairs, the most relevant of which is

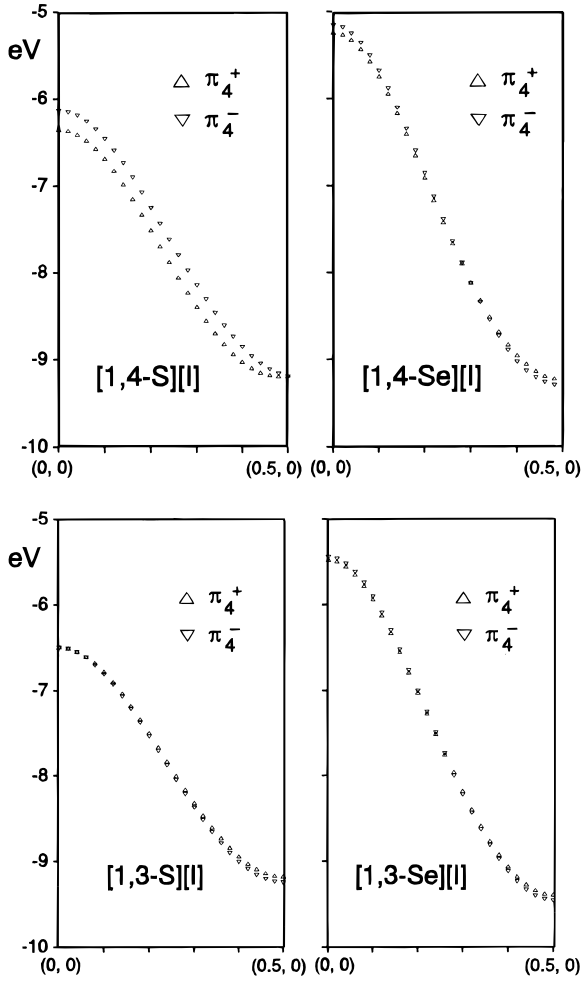

Figure 8. Dispersion of the crystal orbitals π_4^+ and π_4^- along the stacking direction in 2-dimensional models related to [1,4-E][I] and [1,3-E][I] (E = S, Se). The stacking direction is defined as the first dimension.

that arising from the in-phase and out-of-phase combinations of the radical SOMOs π_4^+ and π_4^-. The dispersion of these two orbitals along the stacking direction[18] is shown in Figure 8. It is readily apparent that dispersion is extremely large (3−4 eV), more so for selenium than for sulfur, as expected by virtue of the greater spatial extension of Se 4p orbitals. Dispersion

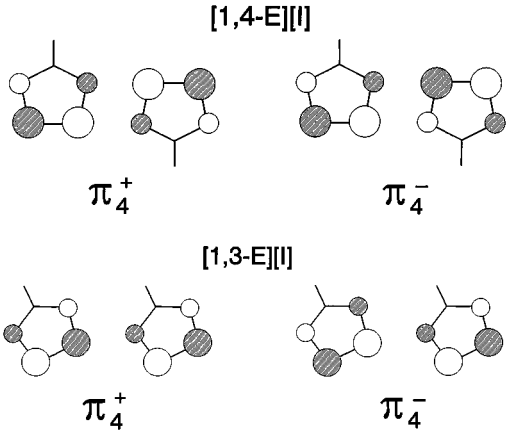

(18) The correspondence of the directions of the reciprocal and real-space vectors is exact for all the structures discussed save [1,4-Se][I]. In [1,4-Se][I] the discussion still retains qualitative value.

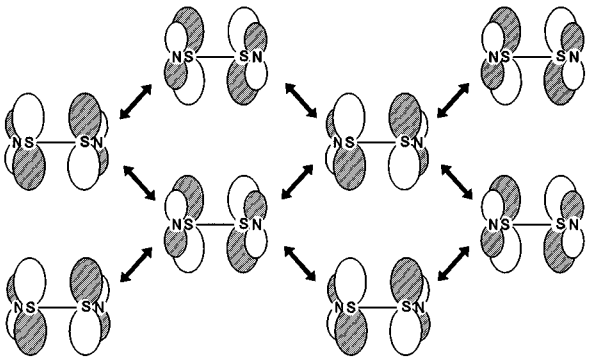

Figure 9. Intercolumnar overlap in π_4^+ in [1,4-S][I] at (0,0). S- - -N overlap is bonding, while S- - -S overlap is antibonding.

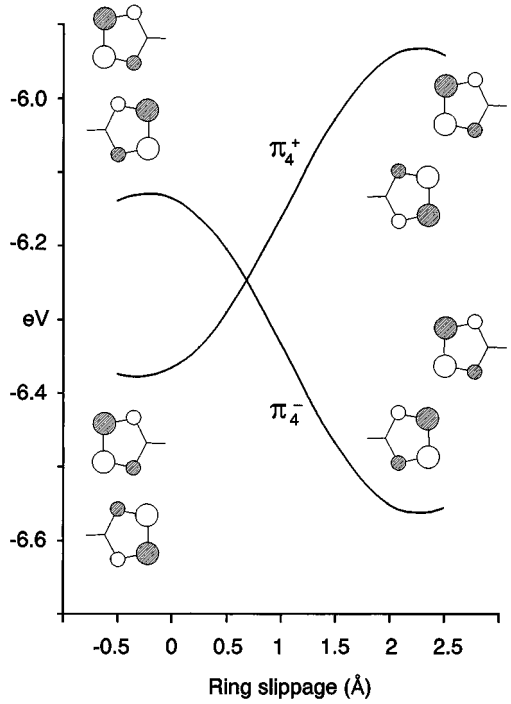

Figure 10. Energies of the crystal orbitals π_4^+ and π_4^- at (0,0) in 2-dimensional models related to [1,4-S][I]. Ring slippage (in angstroms) is defined relative to the observed crystal structure positions.

along the stacking direction is also greater for the 1,4 derivatives compared to the 1,3 compounds, and this we ascribe to the longer cell repeat and consequently weaker interannular overlap in the latter.

Dispersion perpendicular to the stacking direction is small by comparison but is largest in [1,4-S][I], where the separation of the two COs reaches 0.2 eV. Despite the short Se- - -Se and Se- - -N contacts noted for [1,4-Se][I], the two CO combinations are almost coincident in energy. This apparently surprising finding can be attributed in part to the fact that adjacent stacks in [1,4-Se][I] are no longer perfectly out-of-register (Figure 2). More importantly, however, it is a manifestation of the phase properties of the interacting SOMOs. The "dovetailed" packing pattern of the [1,4-E][I] structures leads to close E- - -N contacts, and in [1,4-S][I] these interactions, rather than the S- - -S contacts, are the major contributors to lateral dispersion. Thus, as is illustrated in Figure 10 for the symmetry point (0, 0), π_4^+ lies below π_4^- because the bonding S- - -N interactions outweigh the antibonding S- - -S interactions between adjacent molecules. If S- - -S overlap were dominant, then π_4^- would be more stable than π_4^+. To illustrate further the potential consequences of these opposing S- - -N and S- - -S interactions, we have carried out a model calculation to establish the degree of CO spreading of as a function of a ring slippage (the degree of "dovetailing"). The energy separation of π_4^+ and π_4^- at (0,0) for [1,4-S][I] is plotted as a function of ring slippage in Figure 10. Heavy dovetailing (negative slippage) leads to stabilization of π_4^+ (S- - -N interactions dominate), while less dovetailing (positive slippage) π_4^- lies lower (S- - -S overlap prevails). It is interesting to note that when the slippage is slightly greater than 0.6 Å, these competing effects conspire to nullify any energetic difference between the two COs; dispersion lateral to the stacking direction is completely eliminated.

The structure of [1,4-Se][I] is not orthorhombic, and model calculations on slippage are less easily interpreted. Qualitatively, however, the picture is clear. The structure of [1,4-Se][I] lies close to the crossover point described above, i.e., Se- - -Se overlap is comparable in magnitude (but of opposite sign) to Se- - -N overlap in both π_4^+ and π_4^-, and dispersion lateral to the stacking direction is almost completely suppressed. The higher T_{MI} for [1,4-Se][I] compared to [1,4-S][I] can be understood within this context—the structure is more 1-dimensional, despite (indeed because of) possessing closer E- - -E and E- - -N contacts.

The [1,3-E][I] derivatives are, as expected by inspection of the crystal structures, extremely 1-dimensional. There is virtually no separation in either structure between π_4^+ and π_4^-. This is simply a manifestation of the limited interactions lateral to the stacking direction coupled with the nearly in-register arrangement of stacks, which leads to far poorer overlap characteristics (either E- - -E or E- - -N) between adjacent rings.

Summary

Electrocrystallization provides an effective method for the preparation of iodine-based charge-transfer salts of benzene-bridged bis(diselenadiazolyl) radicals, which cannot be generated in crystalline form by the sublimation methods used previously for their sulfur counterparts. Other phases, e.g., [1,4-Se][I][I_3], can also be generated when high concentrations of iodine are employed. The stacking observed for both sulfur- and selenium-based 1:1 CT iodides lead to extremely wide-band materials which are highly 1-dimensional in nature. The relatively high T_{MI}'s observed for these compounds can be attributed to the absence of 2- and 3-dimensional interactions sufficient to offset the strong tendency of the stacked structure to distort.[19] The generation of more isotropic materials based on these radicals will require the design of molecules in which interactions along the stack are reduced while those transverse to the stack are enhanced. This latter objective will require careful consideration of both the magnitude and phase properties of E- - -E and E- - -N interactions.

Experimental Section

General Procedures and Starting Materials. The starting salts [1,4-Se][SbF_6]$_2$·3PhCN and [1,3-Se][SbF_6]$_2$·

(19) We note, however, that the anisotropies in the conductivity of [1,4-S][I] were suggestive of a relatively isotropic material.

2PhCN were prepared as previously described,[14] i.e., by metathesis of the corresponding dichloride salt with $NOSbF_6$ (Strem), and triple recrystallization from chlorobenzene/benzonitrile. Iodine (Fisher) was resublimed before use. The solvents acetonitrile, benzonitrile, and chlorobenzene were all purified by distillation from P_2O_5. All synthetic and electrochemical work was performed under an atmosphere of nitrogen. Chemical (elemental) analyses were performed by MHW Laboratories, Phoenix, AZ. Infrared spectra of the iodine CT salts could not be obtained because of excessive scattering of the incident radiation by the samples (as Nujol mulls).

Electrocrystallization Experiments. Crystals of [1,4-Se][I] and [1,3-Se][I] suitable for X-ray work and transport property measurements were prepared by electroreduction of 5 mM solutions of $[1,4\text{-Se}][SbF_6]_2 \cdot 3PhCN$ and $[1,3\text{-Se}][SbF_6]_2 \cdot 2PhCN$[20] in acetonitrile (in an H-cell[21] fitted with a D-porosity frit and Pt wire anode and cathode) in the presence of I_2 in the cathode compartment a level of 5 mM (10 mM in I). No supporting electrode was used. Samples for single crystal work were typically grown with a current of 3−5 μA over a period of 10−14 days.[22] Material suitable for bulk analysis was grown at a higher current level, e.g., 5−10 μA. The dark, lustrous needles are stable in air. In view of the fact that no supporting electrolyte was used, no attempt was made to run the cells to exhaustion. Indeed, most electrodeposition experiments cells were halted well before 50% completion.

In the experiments involving the 1,4 derivative, when the concentration of iodine was increased to above 20 mM (40 mM in I) small golden, blocklike crystals of the iodide/triodide salt $[1,4\text{-Se}][I][I_3]$[23] (a room-temperature semiconductor with pressed pellet conductivity near 10^{-1} S cm^{-1}) grew in preference to the needles of [1,4-Se][I]. The use of an indium tin oxide electrode (1 × 3 cm) rather than a Pt wire afforded single crystals of $[1,4\text{-Se}][I][I_3]$ suitable for X-ray work.

X-ray Measurements. All X-ray data were collected on an ENRAF-Nonius CAD-4 diffractometer with monochromated Mo Kα radiation. Crystals were mounted on a glass fiber with silicone rubber. Data were collected using a $\theta/2\theta$ technique. The structures were solved using direct methods and refined by full-matrix least-squares analysis which minimized $\sum w(\Delta F)^2$. A summary of crystallographic data is provided in Table 3.

Magnetic Susceptibility Measurements. The magnetic susceptibilities as a function temperature were measured using a SQUID magnetometer operating at 1 T.

Conductivity Measurements. Four-point conductivity measurements along the highly conducting axes were performed with a Keithley 236 unit. Gold pads were first evaporated onto some of the crystals; wires were attached to the pads with gold paint.

Table 3. Crystal Data

compound	[1,4-Se][I]	[1,3-Se][I]	[1,4-Se][I][I_3]
formula	$ISe_4N_4C_8H_4$	$ISe_4N_4C_8H_4$	$I_4Se_4N_4C_8H_4$
FW	598.88	598.88	979.59
a, Å	10.586(2)	28.489(7)	12.862(3)
b, Å	16.713(2)	3.543(2)	15.063(2)
c, Å	3.5006(14)	12.283(2)	9.028(3)
b, deg	104.26(2)		100.62(2)
V, Å^3	600.2(3)	1239.8(8)	1719.1(7)
d(calcd), g cm^{-3}	3.314	3.21	3.785
space group	$C2/m$	$Ima2$	$C2/c$
Z	2	4	4
λ, Å	0.710 73	0.710 73	0.710 73
temp, K	293	293	293
μ, mm^{-1}	14.63	14.2	15.56
$R(F)$, $R_w(F)^a$	0.028, 0.045	0.047, 0.061	0.059, 0.075
data with $I > 3\sigma(I)$	448	387	769

^{a} $R = [\sum||F_o| - |F_c||]/[\sum|F_o|]$. $R_w = \{[\sum w||F_o| - |F_c||^2]/[\sum(w|F_o|^2)]\}^{1/2}$.

Band Structure Calculations. The band structure calculations were carried out on a 486/66 PC with the EHMACC suite of programs[24] using the parameters discussed previously.[14a,25] The off-diagonal elements of the Hamiltonian matrix were calculated with the standard weighting formula.[26] In the model 2-dimensional calculations the coordinates of the two HCN_2E_2 radicals in the unit cell were taken directly from the X-ray data on [1,4-E][I] and [1,3-E][I] (E = S, Se). To simplify the comparison of the dispersion characteristics of the different structures, the first dimension of the unit cell was defined as the stacking direction. The lateral (cross stack) direction was then set as the second dimension. These choices may not correspond to the crystallographic unit cell directions.

Acknowledgment. Financial support at Guelph was provided by the Natural Sciences and Engineering Research Council of Canada (NSERC) and at Arkansas by the National Science Foundation (EPSCOR program). C.D.B. acknowledges a DOE/ASTA Traineeship, and C.D.M. an NSERC postgraduate scholarship.

Supporting Information Available: Tables of crystal data, structure solution and refinement, and bond lengths and angles (6 pages); anisotropic thermal parameters for the structures reported (17 pages). This material is contained in many libraries on microfiche, immediately follows this article in the microfiche version of the journal, can be ordered from the ACS, and can be downloaded from the Internet; see any current masthead page for ordering information and Internet access instructions.

CM950446S

(20) This salt was prepared in a manner analogous to that for the 1,4 derivative and recrystallized from chlorobenzene/benzonitrile as orange plates. Anal. Calcd for $C_{22}H_{14}N_6F_{12}Se_4Sb_2$: C, 22.98; H, 1.23; N, 7.31%. Found: C, 23.12; H, 1.24; N, 7.50%.

(21) (a) Ferraro, J. R.; Williams, J. M. *Introduction to Synthetic Eleictrical Conductors*; Academic Press: New York, 1987; p 25. (b) Stephens, D. A.; Rehan, A. E.; Compton, S. J.; Barkhau, R. A.; Williams, J. M. *Inorg. Synth.* **1986**, *24*, 135.

(22) Anal. Calcd for $C_8H_4N_4Se_4I$: C, 16.04; H, 0.67; N, 9.36; I, 21.19%. Found for [1,4-Se][I]: C, 15.98; H, 0.73; N, 9.12%; I, 21.41%. Found for [1,3-Se][I]: C, 15.90; H, 0.56; N, 9.16%. The iodine analysis for the latter compounds was variable and irreproducible, as a result of interference from selenium. Repeated and consistent C, H, and N data, plus the iodine occupancy from the X-ray work, confirmed the composition.

(23) The iodine content of this compound was established from the X-ray occupancy factors and by iodine analysis. Calcd for $C_8H_4N_4Se_4I_4$: I, 51.82%. Found: I, 51.98%.

(24) EHMACC, Quantum Chemistry Program Exchange, program number 571.

(25) Basch, H.; Viste, A.; Gray, H. B. *Theor. Chim. Acta* **1965**, *3*, 458.

(26) Ammeter, J. H.; Burghi, H. B.; Thibeault, J. C.; Hoffmann, R. *J. Am. Chem. Soc.* **1978**, *100*, 3686.